SEMARAK ILMU PUBLISHING

Journal of Advanced Research in Fluid Mechanics and Thermal Sciences

Journal homepage:
https://semarakilmu.com.my/journals/index.php/fluid_mechanics_thermal_sciences/index
ISSN: 2289-7879

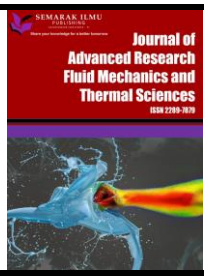

Enhanced The Properties of ZnO Thin Film by Graphene Oxide for Dye Sensitized Solar Cell Applications

Saedah Munirah Sanusi[1], Ruziana Mohamed[1,2,*], Mohd Firdaus Malek[1,2], Nurin Jazlina Ahmad[1], Mohamad Rusop Mahmood[2,3]

[1] Faculty of Applied Sciences, Universiti Teknologi MARA (UiTM), 40450 Shah Alam, Selangor, Malaysia
[2] NANO-SciTech Lab (NST), Centre for Functional Materials and Nanotechnology (FMN), Institute of Science (IOS), Universiti Teknologi MARA (UiTM),40450 Shah Alam, Selangor, Malaysia
[3] NANO-ElecTronic Centre (NET), Faculty of Electrical Engineering, Universiti Teknologi MARA (UiTM), 40450 Shah Alam, Selangor, Malaysia

ARTICLE INFO

Article history:
Received 13 May 2022
Received in revised form 14 October 2022
Accepted 24 October 2022
Available online 13 November 2022

Keywords:
Zinc oxide; graphene oxide; immersion and dye sensitized solar cell

ABSTRACT

In this present work, the effects of coating of graphene oxide (GO) at different concentrations (0, 0.2, 0.3, 0.4, 0.5, and 0.6 mg/ml) onto zinc oxide (ZnO) nanostructured were investigated. ZnO and ZnO coated with GO (ZnO/GO) were prepared using immersion method. The structural, morphology and optical properties of all samples have been studied using x-ray diffraction (XRD), field emission scanning microscopy (FESEM) and UV Vis spectroscopy. The peak obtained from the XRD pattern shows that all samples are in the hexagonal-wurtzite structure. The (002) peak shows the strongest intensity for all samples with the highest (002) peak obtained for the ZnO/GO sample coated at a GO concentration of 0.5 mg/ml. The diameter of ZnO/GO nanostructured samples decreased after coating with GO at concentrations of 0.2 to 0.5 mg/ml and the diameter increased again when ZnO nanostructures were coated with GO at above 0.5 mg/ml. The highest transmission spectrum was obtained for the ZnO/GO sample coated with GO at a concentration of 0.5 mg/ml. In conclusion, the effect of GO coating on ZnO nanostructured can be changed at different concentrations of GO. The optimal properties of ZnO/GO may be suitable as a photoanode in DSSC applications.

1. Introduction

The world's energy consumption is increasing in tandem with population growth. On the other hand, conventional energy resources are rapidly depleting, raising serious concerns about energy crises. To overcome the current issue, attempts are being explored to use renewable energy resources [1]. The dye-sensitized solar cells (DSSC) are the most popular third-generation solar cells that were developed by Grätzel and co-workers in 1991 [2-4]. Nowadays, DSSC has received a lot of attention because of its potential for low-cost solar energy conversion applications.

The DSSC is also known as photovoltaic and exhibits the capability to convert sunlight to electricity. This DSSC has emerged as a promising candidate to harvest energy due to its low-cost

* *Corresponding author.*
E-mail address: ruzianamohd@uitm.edu.my

https://doi.org/10.37934/arfmts.100.3.171181

production, environmentally friendly, high-power conversion efficiency, good performance in diverse light conditions, higher indoor efficiency than silicon solar cells, long-term stability, and stable performance with light intensity [5,6].

The DSSC consists of a semiconductor photoanode, a light-absorbing sensitizer attached to the photoanode's surface, the redox electrolyte, and the counter electrode (CE). Tin oxide (SnO_2), zinc oxide (ZnO), and titanium oxide (TiO_2) are common metal oxides used in the formation of DSSC due to their physical and chemical properties [7]. Commonly, ZnO metal oxide was chosen as a photoanode material over all other metal oxide materials because it has a wide bandgap energy (3.37eV), strong electron mobility (115-155 $cm^2V^{-1}s^{-1}$), high excitation binding energy of 60 meV at ambient temperature, better stability against photo corrosion, and huge surface area [8,9]. The properties of ZnO such as structure, particle size, porosity, and pore size distribution will be affected the electronic device applications. Other than that, ZnO offers several intrinsic advantages, such as a greater electron migration rate, a lower process temperature, and structure can be easily created by varying the parameters process.

However, slow electron injection at the ZnO/dye interface has been reported to be the major limitation of overall photogenerated current in ZnO-based solar cells [10]. Researchers are currently looking at a variety of ways to improve electron transportation in photoelectrodes and reduce charge recombination to enhance the cell performance of ZnO-based DSSC, such as the introduction of materials with high electronic transport and charge carrier mobility. Carbon nanotubes and graphene both have high electrical conductivity and have been introduced into the photoanode of DSSC to improve cell performance by lowering charge recombination [11,12]. Recently, graphene has been identified as a potential candidate for improving dye absorption and carrier transport properties of DSSC [13]. According to Song and Wang [10], the photoelectric conversion efficiency (PCE) of the device could be enhanced by introducing reduced graphene oxide (rGO) into ZnO. The use of graphene increases the porosity of anode films and provides a huge surface area for more dye adsorption sites. Thus, it can increase dye loading and light harvesting efficiency.

Adding graphene oxide (GO) which is one of the graphene derivatives into ZnO will increase the efficiency of DSSC [14-16]. GO is a well-known carbon material that has been the subject of numerous research studies in recent years due to its multifunctional character based on its large surface area, amphiphilicity, and tuneable electronic properties through surface modification [16]. GO is made by oxidizing and exfoliating graphite and consists of a single graphene sheet with conjugated sp2 domains and sp3-like regions. GO contains oxygen functional groups covalently bonded to carbon atoms in the basal plane and on the edges. The chemically active surface of GO allows other organic molecules or metal oxides to attach to it, changing its electrical characteristics. Víctor-Román *et al.,* [17] developed the ZnO-GO hybrids for the degradation of methylene blue under UV-light irradiation. The set of ZnO-GO hybrids has been synthesized in an ultrasonication process involving ZnO nanoparticles [17]. Boukhoubza *et al.,* [18] used the simple hydrothermal process to improve the ZnO NR/GO nanocomposites with different GO amounts. Sha *et al.,* [19] improved the PCE of DSSC by constructing ZnO/rGO photoanode by using one step electrodeposition method.

ZnO nanostructures are commonly synthesized via solvothermal, hydrothermal and sol-gel immersion methods [20]. In the fabrication of nanostructured material, a low- temperature method of preparation is gaining popularity to allow deposition on thermally adjustable substrates. ZnO nanostructured produced by immersion method are well known to be dependent on preparation parameters such as material concentration, deposition temperature, and time. The morphologies and sizes of a ZnO nanostructure are mostly controlled by concentration [21]. The immersion method is one of the processes that operates at low temperature, simple production process, and can produced in large-scale nanostructured on substrates with low energy process.

In our recent work, we used a new approach to prepare ZnO/GO nanostructured using a double solution immersion method. At first, ZnO nanostructured were grown on a glass substrate coated with ZnO seeds layer and followed by GO coating on top of ZnO nanostructured. The structural, morphological and optical properties of ZnO/GO nanostructured were investigated as photoanode in DSSC applications.

2. Methodology

2.1 Growth Process

The preparation of the ZnO doped seeded layer was explained in detail by Mohamed *et al.,* [22]. ZnO/GO nanorod arrays were grown on ZnO seeded layer-coated substrate using the aqueous solution immersion method. Zinc nitrate hexahydrate ($Zn(NO_3)_2).6H_2O$, 98.5%, Riendemann Schmidt) and hexamethylenetetramine ($C_6H_{12}N_4$, 99.5%, HMTA) was used as a precursor and stabilizer, respectively [22]. A measured amount of $Zn(NO_3)_2.6H_2O$ was dissolved in deionized water (DI) to form aqueous solution, and then HMTA was added to the solution. The mixed solution was sonicated under an ultrasonic water bath for 30 min at 50°C. Then, the solution was continuously stirred for 3 hours at room temperature and then poured into a container with an Al: ZnO seed coated glass substrate inserted into the container. The immersion process was done by immersing sealed vessels inside the water bath for 60 minutes at 95°C for nanorod growth [23]. For the second immersion process, GO solution with different concentrations (0, 0.2, 0.3, 0.4, 0.5, and 0.6mg/ml GO) was poured into each vessel onto the ZnO nanorods. The vessels were then immersed again for 20 minutes at 95 °C. DI water was used to rinse the ZnO nanorods and finally, the thin films were annealed at 500°C for 30 minutes in ambient conditions. The as-synthesized ZnO/GO with 0, 0.2, 0.3, 0.4, 0.5 and 0.6mg/ml of GO were labeled as ZnO, ZnO/GO-1, ZnO/GO-2, ZnO/GO-3, ZnO/GO-4, and ZnO/GO-5 respectively. The ZnO/GO nanostructured structure properties were then characterized using x-ray diffraction (XRD) UV-VIS spectroscopy, field emission scanning electron microscope (FESEM), and fourier-transform infrared (FTIR) spectroscopy.

3. Result

3.1 X-ray Diffraction Analysis

The XRD analysis was used to determine the structure and diffraction peaks of samples. XRD patterns of ZnO and ZnO/GO nanostructured at different GO concentrations were presented in Figure 1. The obtained peaks confirm the hexagonal-wurtzite structure for all samples is in good agreement with JCPDS-ICDD card no. 36-1451 [18]. Based on Figure 1, there are three peaks observed for all samples which correspond to (100), (002), and (101) diffraction peaks in the range of 5°–90°. These thin films show a polycrystalline structure that displayed the highest peak intensity at the (002) plane, suggesting the structure was primarily grown along the c-axis or in the direction perpendicular to the substrate on the seed layer [24,25]. The relative peak intensity of the nanostructured was calculated using Eq. (1) [26].

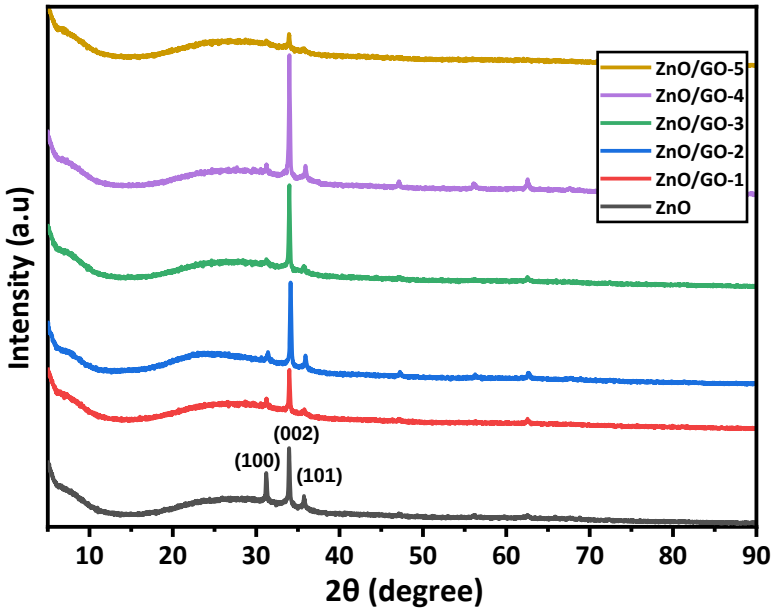

Fig. 1. XRD pattern for ZnO and ZnO/GO nanostructured at different GO concentrations

$$P_{(hkl)} = \frac{I_{(hkl)}}{\Sigma I_{(hkl)}} \quad (1)$$

where I(hkl) is the measured relative intensity for (002) plane and ΣI(hkl) is the intensity of all the diffraction peaks in all plane. The relative peak intensities of the (002) planes are shown in Table 1.

Table 1
The 2Θ peak, FWHM, crystallite size and peak intensity related to the samples

Samples	FWHM (degree)	Crystallite size (nm)	Peak Intensity	Dislocation density, δ ($\frac{Lines}{m^2}$)	Interplanar distance, d (Å)
ZnO	0.19	46.00	0.48	4.77×10^{14}	2.63
ZnO/GO-1	0.19	44.00	0.51	5.21×10^{14}	2.63
ZnO/GO-2	0.21	42.00	0.60	5.80×10^{14}	2.63
ZnO/GO-3	0.23	38.00	0.64	6.96×10^{14}	2.64
ZnO/GO-4	0.24	36.00	0.67	7.59×10^{14}	2.64
ZnO/GO-5	0.18	47.00	0.41	4.52×10^{14}	2.64

According to the estimated values, the relative peak intensity of the (002) peak increases as the concentration of GO coated on ZnO nanorods increases. The relative peak intensity of ZnO/GO nanostructured improves from 0.2- 0.5 mg/ml of GO concentration. This implies that the ZnO/GO-4 nanostructured sample has the highest relative peak intensity along the c-axis and better crystallinity than other samples. Thus, it is this sample nanostructured might be suitable for ZnO-based photoanode. The higher relative peak intensity along the c-axis presents good crystallographic planes and nanostructured formation at minimum surface energy. However, the intensity of the peak ZnO/GO nanostructured decreased with further addition of at 0.6 mg/ml of GO concentration. This reduction behavior in the crystallinity of ZnO/GO structure might be due to the uniformity structure and increase of grain boundary of nanostructured when coated with GO over 0.5 mg/ml concentration. The full-width half-maximum (FWHM) values of the nanostructured are around 0.24 and 0.18 respectively. Diffraction peaks of GO were not found due to its small amount. The absence

of typical diffraction peaks of GO stacking layers could be attributed to the fact that introducing ZnO into the sheets of GO destroys the regular stacking of GO layers [27].

The average crystallite size of nanostructured samples can be estimated from Debye-Scherer's Eq. (2).

$$D = \frac{0.94\lambda}{\beta cos\theta} \tag{2}$$

The crystallite size of ZnO/GO nanostructured decreases when concentration of GO coated on ZnO nanorods increases. The smallest crystallite size was shown by ZnO/GO-4. Chava and Kang [28] reported that, as the crystal size decreases, smaller particle sizes can be obtained. Therefore, in electronic applications such as DSSC, a smaller particle size of samples is good to be used for the absorption of dyes due to a large surface area [28]. It obviously indicates that ZnO/GO-4 has a large internal surface area for more dye loading. In general, a more dye-loaded photoanode harvests more photons from incident light, resulting in a higher Jsc [29]. Dislocation density, δ of the nanostructured is estimated from crystalline size using Eq. (3).

$$\delta = \frac{1}{D^2} \tag{3}$$

where D(002) is the crystallite size. The dislocation density of ZnO and ZnO/GO nanostructured increase by GO coating concentration from 0 to 0.5 mg/ml. Because of the introduction of defects such as oxygen vacancies and zinc interstitials, stress and strain have a significant impact on the film properties. According to Bragg's equation, the inter-planar distances of the diffracting planes d and the lattice constants a and c of wurtzite structure films were determined using Eq. (4) [26]:

$$2d_{hkl}\ \sin\theta = n\lambda \tag{4}$$

where d_{hkl} is the distance between lattice planes of Miller indices (h, k, and l), n is the order of diffraction (usually n=1), λ is the X-ray wavelength of CuKα radiation (1.54 Å) and θ is Bragg's angle (half of the peak position angle).

3.2 Field Emission Scanning Electron Microscope (FESEM)

The FESEM images in Figure 2 show that all the samples were grown vertically aligned hexagonal structures on the glass substrate ZnO seed layer. The coating of GO at different concentration from 0 - 0.5 mg/ml indeed influences the ZnO nanorods growth by reducing the size of nanorods from 104 to 56 nm, respectively (Table 2). The size of ZnO nanorods decrease when concentration of GO coating increase over 0.5 mg/ml. It was found that ZnO/GO-4 sample has the smallest size with better distribution of nanostructured. Atanacio-Sánchez *et al.,* [7] discovered that a sample with greater distribution of particles has the highest efficiency of DSSC. The decrease in the diameter of the nanorods could be attributed to the cleavage of some larger nanorods and the surface area of the thin film can increase [18]. A larger surface area will cause more dye molecules to be absorbed onto the surface of the nanostructure. Thus, it will produce more current and might be suitable to increase power conversion efficiency for DSSC [18,30].

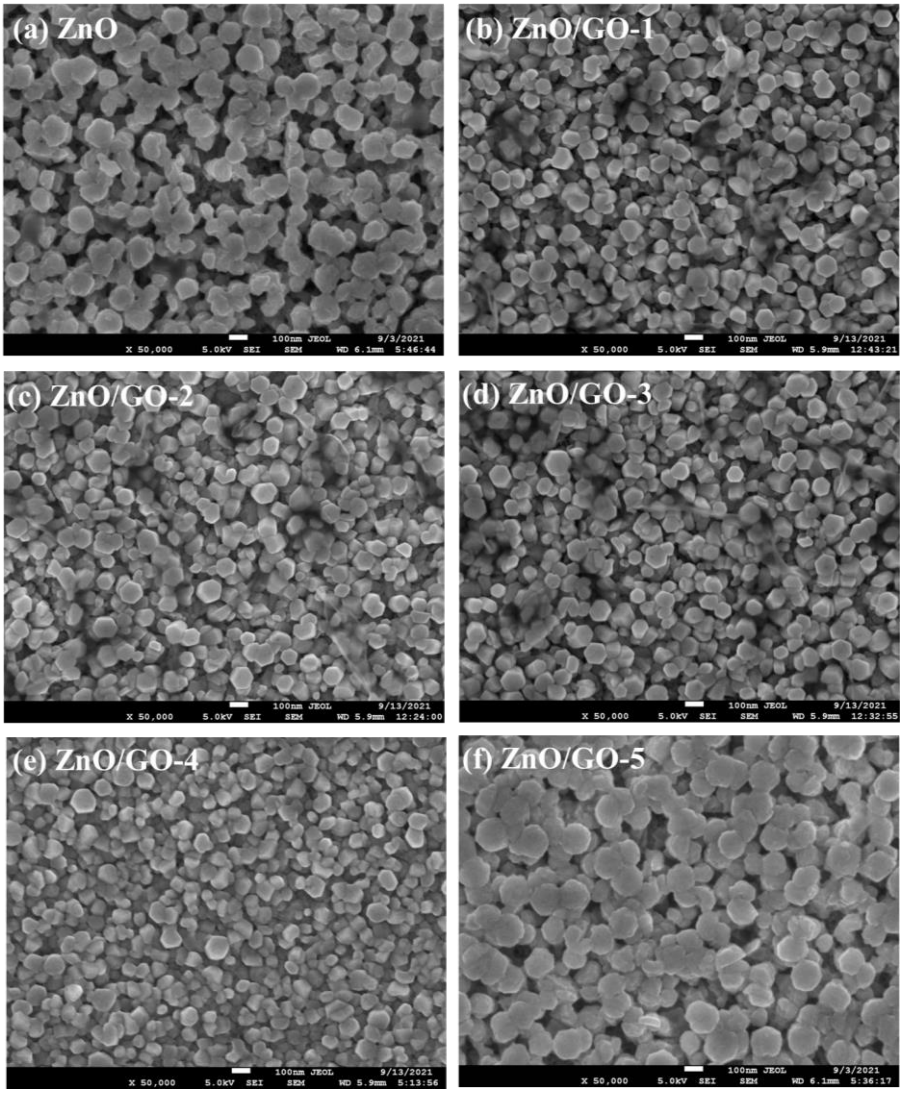

Fig. 2. FESEM micrograph of (a) ZnO, (b) ZnO/GO-1, (c) ZnO/GO-2, (d) ZnO/GO-3, (e) ZnO/GO-4 and (f) ZnO/GO-5 thin films

Table 2
The average diameter of all the thin films

Samples	Average Diameter (nm)
ZnO	104
ZnO/GO-1	74
ZnO/GO-2	69
ZnO/GO-3	67
ZnO/GO-4	56
ZnO/GO-5	113

3.3 Fourier-Transform Infrared (FTIR) Spectroscopy

The surface functional groups in ZnO and ZnO/GO nanostructured were studied using FTIR spectroscopy as shown in Figure 3. The oxygen functional group peaks in the ZnO/GO sample are found at 1071, 1178, and 1730 cm^{-1} which correspond to C–O stretching vibrations, C–OH stretching, and sp2-hybridized C=C groups, respectively. The appearance of new peaks between 600 and 1180 cm^{-1} can be attributed to Zn-C stretching bonding. Any shift or change in the position and intensity

of peaks in the FTIR spectra of samples indicates the contribution of functional groups of GO with ZnO nanorods [31]. Broadband in 1080 cm^{-1} is observed as part of the nature of the C– O–C stretching vibration of some residual chemical agent in the ZnO and ZnO–GO, which is why the stretching vibration is more pronounced in the ZnO–OH. Furthermore, as can be seen, the ZnO/GO samples exhibit a stronger downward disturbance than the ZnO. This disturbance is caused by more energy being absorbed, which may be due to particle size [7,32].

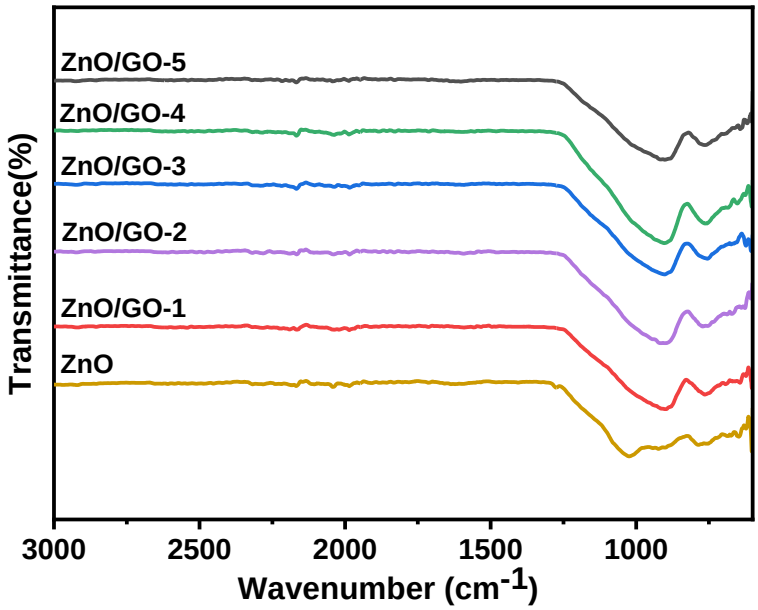

Fig. 3. FTIR spectra of ZnO, and ZnO/GO thin films

3.4 UV-visible Analysis

3.4.1 Transmittance

The transmittance spectrum of ZnO and ZnO/GO samples are presented in Figure 4. The transmittance spectrum increases with increasing of GO coating concentration from 0 to 0.5 mg/ml that presented by ZnO to ZnO/GO-4, respectively. Decrease of transmittance for ZnO/GO-5 nanostructured occurred at higher GO coating concentration which is over than 0.5 mg/ml. The increase in transmission spectrum may be related to the increase in carrier concentration in ZnO/GO nanostructured due to the high degree of vertical alignment, low surface roughness, and uniformity of ZnO/GO nanostructured [22]. The transmission dropped dramatically near the visible region, which corresponded to the intrinsic bandgap energy of ZnO [33]. The reduction of transmittance is attributed to the structural properties and film thickness [34]. Previous research suggests that ZnO film transmittance decreases as the nanostructured size decreases [35]. The porosity of the ZnO thin films can be calculated using the following Eq. (5) [28]:

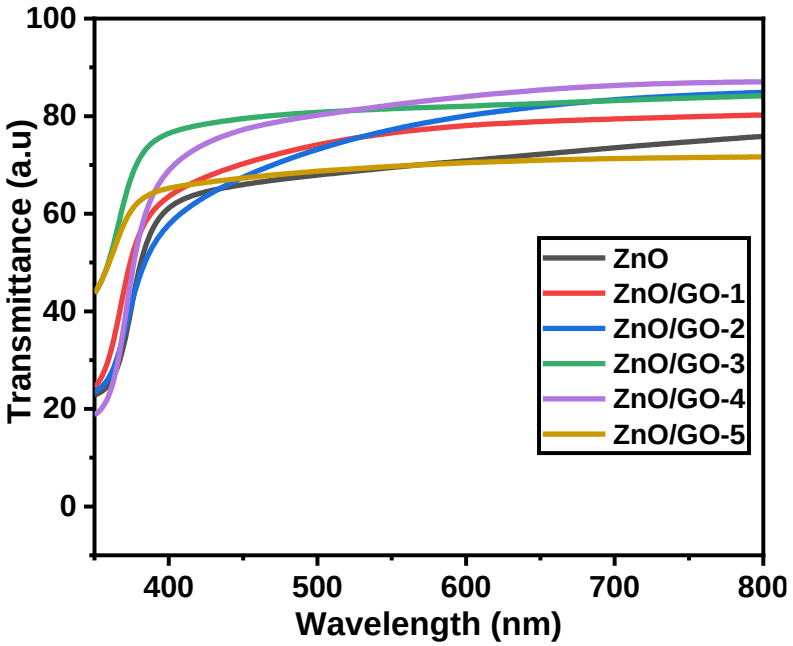

Fig. 4. Comparison of the optical transmittance of ZnO thin films for various GO concentrations

$$\text{Porosity} = 1 - \frac{\left(\frac{n_f^2-1}{n_f^2+2}\right)}{\left(\frac{n_s^2-1}{n_s^2+2}\right)} \quad (5)$$

where n_f is the refractive index of the porous ZnO films and n_s is the widely accepted refractive index of the ZnO skeleton, which is 2. The following equations are used to calculate the refractive index, nf, in the transmittance region where the absorption coefficient, 0.

$$n_f = [N + (N^2 + S^2)^{1/2}]^{1/2} \quad (6)$$

$$N = \frac{2S}{T_m} - \frac{(S^2+1)}{2} \quad (7)$$

Tm is the envelope function of the maximum and minimum transmittance values, and S is the substrate's refractive index, which in this case is 1.52 for the transparent glass substrate. The Tm value can be calculated by averaging the transmittance data from the transparent region between 400 and 800nm wavelength or where the value is close to 0. ZnO/GO-4 shows the highest porosity state that may be attributed to good transmissibility for dye adsorption and can improve electrolyte ion exchange rates, reducing recombination losses and increasing conversion efficiencies (Table 3) [36]. As mentioned by Ghann *et al.,* [37], the porous surface of the material of photoanode suggests an enhancement in the adsorption of dye into the ZnO structure.

Table 3
The average transmittance and porosity of ZnO thin films with different GO concentrations

Samples	Average Transmittance	Porosity (%)
ZnO	70.4921	1.3045
ZnO/GO-1	76.2186	1.3054
ZnO/GO-2	77.4929	1.3055
ZnO/GO-3	81.7557	1.3058
ZnO/GO-4	82.6607	1.3060
ZnO/GO-5	68.4822	1.3042

4. Conclusions

In summary, we have successfully prepared the ZnO/GO nanostructured thin films via double step solution immersion method. The XRD pattern indicates that ZnO and ZnO/GO thin films present a hexagonal wurtzite structure, which preferentially grows along the (002) orientation. The ZnO/GO-4 thin film gives the smallest crystallite size which is around and diameter. The FESEM images indicated the hexagonal shape of all samples with the smallest diameter (56 nm) shown by ZnO/GO-4 sample. The highest transmittance spectrum is shown by ZnO/GO-4 which might be due to the increase in carrier concentration in ZnO/GO nanostructured due to the high degree of vertical alignment, low surface roughness, and uniformity of ZnO/GO nanostructured. These findings demonstrate that the coating ZnO with GO improves the properties of ZnO nanostructured and the optimal sample might be suitable to be used as a photoanode in DSSC.

Acknowledgement
The authors would like to acknowledge the Ministry of Education for the financial support of this project (FRGS 600-IRMI/FRGS 5/3 (264/2019). The authors gratefully acknowledge the Research Management Institute (RMI) of UiTM, Nano SciTech Lab (NST), Faculty Applied Sciences of UiTM and Ins. of Graduate Studies (IPSIS) of UiTM for providing laboratory facilities and financial assistance for this study.

References
[1] Lubis, Hamzah. "Renewable Energy of Rice Husk for Reducing Fossil Energy in Indonesia." *Journal of Advanced Research in Applied Sciences and Engineering Technology* 11, no. 1 (2018): 17-22.
[2] Jeong, Woo-Seok, Jin-Wook Lee, Soonil Jung, Jae Ho Yun, and Nam-Gyu Park. "Evaluation of external quantum efficiency of a 12.35% tandem solar cell comprising dye-sensitized and CIGS solar cells." *Solar Energy Materials and Solar Cells* 95, no. 12 (2011): 3419-3423. https://doi.org/10.1016/j.solmat.2011.07.038
[3] Kamat, Prashant V. "Quantum dot solar cells. The next big thing in photovoltaics." *The Journal of Physical Chemistry Letters* 4, no. 6 (2013): 908-918. https://doi.org/10.1021/jz400052e
[4] Gao, Feng, Chuan-Lu Yang, Mei-Shan Wang, Xiao-Guang Ma, and You-Gen Yi. "Theoretical insight on the nanocomposite of tetraphenylporphyrin-graphene oxide quantum dot as a sensitizer of DSSC." *Journal of Photochemistry and Photobiology A: Chemistry* 379 (2019): 24-31. https://doi.org/10.1016/j.jphotochem.2019.05.002
[5] Hug, Hubert, Michael Bader, Peter Mair, and Thilo Glatzel. "Biophotovoltaics: natural pigments in dye-sensitized solar cells." *Applied Energy* 115 (2014): 216-225. https://doi.org/10.1016/j.apenergy.2013.10.055
[6] Xue, Yuhua, Jun Liu, Hao Chen, Ruigang Wang, Dingqiang Li, Jia Qu, and Liming Dai. "Nitrogen-doped graphene foams as metal-free counter electrodes in high-performance dye-sensitized solar cells." *Angewandte Chemie International Edition* 51, no. 48 (2012): 12124-12127. https://doi.org/10.1002/anie.201207277
[7] Atanacio-Sánchez, X., W. J. Pech-Rodríguez, E. N. Armendáriz-Mireles, J. A. Castillo-Robles, P. C. Meléndez-González, and E. Rocha-Rangel. "Improving performance of ZnO flexible dye sensitized solar cell by incorporation of graphene oxide." *Microsystem Technologies* 26, no. 12 (2020): 3591-3599. https://doi.org/10.1007/s00542-020-04820-x

[8] Golsheikh, Amir Moradi, Khosro Zangeneh Kamali, Nay Ming Huang, and Ali Khorsand Zak. "Effect of calcination temperature on performance of ZnO nanoparticles for dye-sensitized solar cells." *Powder Technology* 329 (2018): 282-287. https://doi.org/10.1016/j.powtec.2017.11.065

[9] Hamrayev, Hemra, Kamyar Shameli, and Mostafa Yusefi. "Preparation of zinc oxide nanoparticles and its cancer treatment effects: A review paper." *Journal of Advanced Research in Micro and Nano Engineering* 2, no. 1 (2020): 1-11.

[10] Song, Jun-Ling, and Xiu Wang. "Effect of incorporation of reduced graphene oxide on ZnO-based dye-sensitized solar cells." *Physica E: Low-dimensional Systems and Nanostructures* 81 (2016): 14-18. https://doi.org/10.1016/j.physe.2016.02.005

[11] Batmunkh, Munkhbayar, Mark J. Biggs, and Joseph G. Shapter. "Carbon nanotubes for dye-sensitized solar cells." *Small* 11, no. 25 (2015): 2963-2989. https://doi.org/10.1002/smll.201403155

[12] Li, Fen, Xue Jiang, Jijun Zhao, and Shengbai Zhang. "Graphene oxide: A promising nanomaterial for energy and environmental applications." *Nano Energy* 16 (2015): 488-515. https://doi.org/10.1016/j.nanoen.2015.07.014

[13] Tang, Bo, Guoxin Hu, Hanyang Gao, and Zixing Shi. "Three-dimensional graphene network assisted high performance dye sensitized solar cells." *Journal of Power Sources* 234 (2013): 60-68. https://doi.org/10.1016/j.jpowsour.2013.01.130

[14] Nien, Yu-Hsun, Huang-Hua Chen, Hui-Hsuan Hsu, Po-Yu Kuo, Jung-Chuan Chou, Chih-Hsien Lai, Geng-Ming Hu, Chien-Hung Kuo, and Cheng-Chu Ko. "Enhanced photovoltaic conversion efficiency in dye-sensitized solar cells based on photoanode consisting of TiO_2/GO/Ag nanofibers." *Vacuum* 167 (2019): 47-53. https://doi.org/10.1016/j.vacuum.2019.05.022

[15] Wei, Liguo, Ping Wang, Yulin Yang, Zhaoshun Zhan, Yongli Dong, Weina Song, and Ruiqing Fan. "Enhanced performance of the dye-sensitized solar cells by the introduction of graphene oxide into the TiO_2 photoanode." *Inorganic Chemistry Frontiers* 5, no. 1 (2018): 54-62. https://doi.org/10.1039/C7QI00503B

[16] Ramli, Ahmad Muslihin, Mohd Zikri Razali, and Norasikin Ahmad Ludin. "Performance enhancement of dye sensitized solar cell using graphene oxide doped titanium dioxide photoelectrode." *Malaysian Journal of Analytical Sciences* 21, no. 4 (2017): 928-940. https://doi.org/10.17576/mjas-2017-2104-20

[17] Víctor-Román, Sandra, Enrique García-Bordejé, Javier Hernández-Ferrer, José M. González-Domínguez, Alejandro Ansón-Casaos, Adrián MT Silva, Wolfgang K. Maser, and Ana M. Benito. "Controlling the surface chemistry of graphene oxide: Key towards efficient ZnO-GO photocatalysts." *Catalysis Today* 357 (2020): 350-360. https://doi.org/10.1016/j.cattod.2019.05.049

[18] Boukhoubza, Issam, Mohammed Khenfouch, Mohamed Achehboune, Liviu Leontie, Aurelian Catalin Galca, Monica Enculescu, Aurelian Carlescu et al. "Graphene oxide concentration effect on the optoelectronic properties of ZnO/GO nanocomposites." *Nanomaterials* 10, no. 8 (2020): 1532. https://doi.org/10.3390/nano10081532

[19] Sha, Simiao, Hui Lu, Shaolin Yang, Tong Li, Jiandong Wu, Jinfu Ma, Kang Wang, Chunping Hou, Zhilin Sheng, and Yingchun Li. "One-step electrodeposition of ZnO/graphene composite film as photoanode for dye-sensitised solar cells." *Colloids and Surfaces A: Physicochemical and Engineering Aspects* 630 (2021): 127491. https://doi.org/10.1016/j.colsurfa.2021.127491

[20] Suriani, A. B., A. Mohamed, N. Hashim, M. S. Rosmi, M. H. Mamat, M. F. Malek, M. J. Salifairus, and HPS Abdul Khalil. "Reduced graphene oxide/platinum hybrid counter electrode assisted by custom-made triple-tail surfactant and zinc oxide/titanium dioxide bilayer nanocomposite photoanode for enhancement of DSSCs photovoltaic performance." *Optik* 161 (2018): 70-83. https://doi.org/10.1016/j.ijleo.2018.02.013

[21] Azlinda, Ab Aziz, Zuraida Khusaimi, Mohd Husairi Fadzilah Suhaimi, Nor Iyazi Nasruddin, S. Abdullah, and Mohamad Rusop. "Annealing effect on the surface morphology and photoluminescence properties of ZnO hexagonal rods by immersion method." In *Advanced Materials Research*, vol. 576, pp. 353-356. Trans Tech Publications Ltd, 2012. https://doi.org/10.4028/www.scientific.net/AMR.576.353

[22] Mohamed, R., M. H. Mamat, A. S. Ismail, M. F. Malek, A. S. Zoolfakar, Z. Khusaimi, A. B. Suriani, A. Mohamed, M. K. Ahmad, and M. Rusop. "Hierarchically assembled tin-doped zinc oxide nanorods using low-temperature immersion route for low temperature ethanol sensing." *Journal of Materials Science: Materials in Electronics* 28, no. 21 (2017): 16292-16305. https://doi.org/10.1007/s10854-017-7535-9

[23] Saurdi, I., M. H. Mamat, M. F. Malek, and M. Rusop. "Preparation of aligned ZnO nanorod arrays on Sn-doped ZnO thin films by sonicated sol-gel immersion fabricated for dye-sensitized solar cell." *Advances in Materials Science and Engineering* 2014 (2014). https://doi.org/10.1155/2014/636725

[24] Asib, N. A. M., F. S. Husairi, K. A. Eswar, A. N. Afaah, M. H. Mamat, M. Rusop, and Z. Khusaimi. "Developing high-sensitivity UV sensors based on ZnO nanorods grown on TiO_2 seed layer films using solution immersion method." *Sensors and Actuators A: Physical* 302 (2020): 111827. https://doi.org/10.1016/j.sna.2019.111827

[25] Mamat, M. H., Z. Khusaimi, M. Z. Musa, M. F. Malek, and M. Rusop. "Fabrication of ultraviolet photoconductive sensor using a novel aluminium-doped zinc oxide nanorod-nanoflake network thin film prepared via ultrasonic-

assisted sol-gel and immersion methods." *Sensors and Actuators A: Physical* 171, no. 2 (2011): 241-247. https://doi.org/10.1016/j.sna.2011.07.002

[26] Malek, M. F., M. H. Mamat, M. Z. Musa, Z. Khusaimi, M. Z. Sahdan, A. B. Suriani, A. Ishak, I. Saurdi, S. A. Rahman, and M. Rusop. "Thermal annealing-induced formation of ZnO nanoparticles: Minimum strain and stress ameliorate preferred c-axis orientation and crystal-growth properties." *Journal of Alloys and Compounds* 610 (2014): 575-588. https://doi.org/10.1016/j.jallcom.2014.05.036

[27] Chen, Ya-Li, Chun-E. Zhang, Chao Deng, Peng Fei, Ming Zhong, and Bi-Tao Su. "Preparation of ZnO/GO composite material with highly photocatalytic performance via an improved two-step method." *Chinese Chemical Letters* 24, no. 6 (2013): 518-520. https://doi.org/10.1016/j.cclet.2013.03.034

[28] Chava, Rama Krishna, and Misook Kang. "Improving the photovoltaic conversion efficiency of ZnO based dye sensitized solar cells by indium doping." *Journal of Alloys and Compounds* 692 (2017): 67-76. https://doi.org/10.1016/j.jallcom.2016.09.029

[29] Marimuthu, T., N. Anandhan, R. Thangamuthu, and S. Surya. "Facile growth of ZnO nanowire arrays and nanoneedle arrays with flower structure on ZnO-TiO_2 seed layer for DSSC applications." *Journal of Alloys and Compounds* 693 (2017): 1011-1019. https://doi.org/10.1016/j.jallcom.2016.09.260

[30] Lai, Yi-Hsuan, Chia-Yu Lin, Hsin-Wei Chen, Jian-Ging Chen, Chung-Wei Kung, R. Vittal, and Kuo-Chuan Ho. "Fabrication of a ZnO film with a mosaic structure for a high efficient dye-sensitized solar cell." *Journal of Materials Chemistry* 20, no. 42 (2010): 9379-9385. https://doi.org/10.1039/c0jm01787f

[31] Alamdari, Sanaz, Morteza Sasani Ghamsari, Hosein Afarideh, Aghil Mohammadi, Shayan Geranmayeh, Majid Jafar Tafreshi, and Mohammad Hosein Ehsani. "Preparation and characterization of GO-ZnO nanocomposite for UV detection application." *Optical Materials* 92 (2019): 243-250. https://doi.org/10.1016/j.optmat.2019.04.041

[32] Joseph, Siby, and Beena Mathew. "Microwave-assisted green synthesis of silver nanoparticles and the study on catalytic activity in the degradation of dyes." *Journal of Molecular Liquids* 204 (2015): 184-191. https://doi.org/10.1016/j.molliq.2015.01.027

[33] Malek, M. F., M. H. Mamat, Z. Khusaimi, M. Z. Sahdan, M. Z. Musa, A. R. Zainun, A. B. Suriani, N. D. Md Sin, S. B. Abd Hamid, and M. Rusop. "Sonicated sol-gel preparation of nanoparticulate ZnO thin films with various deposition speeds: The highly preferred c-axis (002) orientation enhances the final properties." *Journal of Alloys and Compounds* 582 (2014): 12-21. https://doi.org/10.1016/j.jallcom.2013.07.202

[34] Valanarasu, S., V. Dhanasekaran, M. Karunakaran, T. A. Vijayan, I. Kulandaisamy, R. Chandramohan, K. K. LEEe, and T. Mahalingam. "Optical and microstructural properties of sol-gel spin coated $MgAl_2O_4$ thin films." *Digest Journal of Nanomaterials and Biostructures* 10, no. 2 (2015): 643-654.

[35] Lu, Wei-Lun, Pin-Kun Hung, Chen-I. Hung, Chih-Hung Yeh, and Mau-Phon Houng. "Improved optical transmittance of Al-doped ZnO thin films by use of ZnO nanorods." *Materials Chemistry and Physics* 130, no. 1-2 (2011): 619-623. https://doi.org/10.1016/j.matchemphys.2011.07.034

[36] Chen, Lung-Chien, Chih-Hung Hsu, Po-Shun Chan, Xiuyu Zhang, and Cing-Jhih Huang. "Improving the performance of dye-sensitized solar cells with TiO_2/graphene/TiO_2 sandwich structure." *Nanoscale Research Letters* 9, no. 1 (2014): 1-7. https://doi.org/10.1186/1556-276X-9-380

[37] Ghann, William, Hyeonggon Kang, Tajbik Sheikh, Sunil Yadav, Tulio Chavez-Gil, Fred Nesbitt, and Jamal Uddin. "Fabrication, optimization and characterization of natural dye sensitized solar cell." *Scientific Reports* 7, no. 1 (2017): 1-12. https://doi.org/10.1038/srep41470